Effects of EPDM and Wollastonite on Structure of Isotactic Polypropylene Blends and Composites

Ivan Šmit,[1] Vojko Musil,[2] Iztok Švab[2]

[1]*Ruđer Bošković Institute, Bijenička 54, P.O. Box 180, 10002 Zagreb, Croatia*
[2]*University of Maribor, EPF Maribor, Institute for Technology, Razlagova 14, 2000 Maribor, Slovenia*

Received 31 January 2003; accepted 8 July 2003

ABSTRACT: Polypropylene blends and composites with 5, 10, and 15 vol % of EPDM and 2, 4, and 6 vol % of untreated and treated wollastonite filler were examined by applying different techniques. Elastomeric ethylene/propylene/diene terpolymer (EPDM) component and wollastonite influenced the crystallization process of isotactic polypropylene (iPP) matrix in different ways. The nucleation of hexagonal β-iPP, the increase of overall degree of crystallinity, and crystallite size of iPP were more strongly affected by wollastonite than the addition of EPDM was. Both ingredients also differently influenced the orientation of α-form crystals in iPP matrix. Wollastonite increased the number of a^*-axis-oriented α-iPP lamellae plan parallel to the sample surface, whereas the addition of EPDM reoriented the lamellae. The orientation parameters of ternary composites exhibited intermediate values between those for binary systems because of the effects of both components. EPDM elastomer considerably affected well-developed spherulitization of iPP, increasing the spherulite size. Contrary to EPDM, because of nucleating ability or crystal habit, wollastonite caused significantly smaller iPP spherulites. Small spherulites in ternary iPP/EPDM/wollastonite composites indicated that the wollastonite filler (even in smallest amounts) exclusively determined the morphology of ternary composites. © 2004 Wiley Periodicals, Inc. J Appl Polym Sci 91: 4072–4081, 2004

Key words: polypropylene blends; polypropylene composites; phase structure; phase morphology; ethylene/propylene/diene terpolymer; wollastonite

INTRODUCTION

The incorporation of inorganic fillers improves some mechanical properties of polymers such as stiffness, hardness, and strength; it might reduce some degradation processes in polymers. Furthermore, it modifies heat distortion temperature, flame retardancy, and electrical properties, as well as makes the production of polymers less costly. The fillers affect ultimate mechanical properties in the two following ways: (1) they act directly as harder particles with determined properties (shape, size, and modulus); and (2) they affect crystallization processes in polymer matrix and ultimate phase structure and morphology of semicrystalline polymer. Among several fillers used for isotactic polypropylene (iPP) is a suitable mineral, wollastonite, $CaSiO_3$ (calcium metasilicate). Because of acicular crystal habit (high aspect ratio $L/D = 10:1 \cdots 20:1$) and its relatively high hardness (according to Mohs: 4.5), wollastonite gives polymer composites reinforcing properties.[1–3] However, its use is limited by restricted sources (only two deposits).[2] In the last decade, investigations have shown that wollastonite acts as a β-nucleator and a reinforcement for iPP.[4–14] The wollastonite-filled iPP improves mechanical properties (scratch and mar resistance) and offers heat-aging characteristics better than those obtained in talc-filled iPP.[11,12,14]

The weaknesses of stiff fillers incorporation such as wollastonites in iPP/$CaSiO_3$ composites are ascribed to the reduced toughness of polymer and poor impact strength of iPP at low temperatures. The above disadvantages can be compensated for by the addition of a soft elastomer component, which can encapsulate filler particles and enhances impact resistance. An effective elastomer modifier should either have a similar interlayer block component or be able to act with the chains of matrix iPP phase. The elastomer interphase, which acts as an adhesive and bumper interlayer, absorbs the impact energy and enhances composite strength. The ethylene/propylene/diene terpolymer (EPDM) is one of the best impact modifiers for iPP. Some extensive research of iPP/EPDM blends is cited in recent reviews.[15–17] Because of the variety of ternary iPP/elastomer/filler composites properties, they could be used for many different applications.[18–20]

The purpose of this work was to investigate the effects of a varying content of wollastonite (with either treated or untreated surfaces) and the EPDM elas-

Correspondence to: I. Šmit (ismit@rudjer.irb.hr).
Contract grant sponsor: Ministry of Science and Technology of the Republic of Slovenia.
Contract grant sponsor: Ministry of Science and Technology of the Republic of Croatia.

tomer in iPP matrix upon the structure of iPP/EPDM/wollastonite composites.

EXPERIMENTAL

Materials

The polymers used in this study were as follows: iPP Novolen 1100L, BASF, Germany (melt flow ratio [MFR] = 5 g/10 min, ρ = 0.908 g/cm^3) and EPDM (Dutral TER 4038, Montedison, Italy; Mooney viscosity ML (1 + 4) 394 K = 65, ρ = 0.865 g/cm^3). Applied mineral fillers were untreated calcium metasilicate, wollastonite (in text $CaSiO_3$; Tremin 939 300 PST, Quarzwerke, Frechon, Germany), and wollastonite treated with aminosilanes (Tremin 939 300 ASTF; in text $CaSiO_3^*$). The applied wollastonites were of the following general characteristics: ρ = 2.85 g/cm^3, d(50%) = 10 μm, specific surface = 1.2 m^2/g, hardness (Mohs) = 4.5.

Blends and composites preparation

The components for the iPP/EPDM blends, binary iPP/wollastonite, and ternary iPP/EPDM/wollastonite composites were premixed by tumble blending and subsequently melt-blended in a Brabender kneading chamber at 473 K for 15 min with a rotor speed of 60 rpm. After homogenization, the blends and composites were compression molded in a preheated hydraulic press (at 473 K) into 1-mm-thick plates. The amounts of EPDM in the iPP blends and composites samples were 5, 10, and 15 vol %, whereas the amounts of treated and untreated wollastonite in composites were 2, 4, and 6 vol %.

Wide-angle x-ray diffraction (waxd)

The wide-angle X-ray diffractograms of rotated samples (1-mm-thick plates) were taken by a Philips diffractometer with monochromatized CuKα radiation in the diffraction range of 2Θ = 4–50°. A degree of crystallinity, $w_{c,x}$, was evaluated by the Hermans–Weidinger method,[21] by using an angular range of 2Θ = 6–34°. Theoretical values of degree of crystallinity ($w_{c,\mathrm{calc}}$) were calculated by the additivity rule[22]

$$w_{c,\mathrm{calc}} = w_{c,x,1} f_1 + w_{c,x,2}(1 - f_1) \quad (1)$$

where $w_{c,x,1}$ and $w_{c,x,2}$ were crystallinities of polymers 1 and 2 in the blend, whereas f_1 was the weight fraction of polymer 1.

From half-maximum width of *110* and *040* reflections, the crystallite sizes L_{110} and L_{040} were calculated by Scherrer formula[23] after the correction for instrumental broadening with a *111*-germanium diffraction profile. The orientation parameters A_{110}, A_{130}, and C, used as measures for orientations of corresponding (110), (130) and (040) planes, were calculated by formulae proposed by Trotignon and Verdu[24] and Zipper et al.[25]:

$$A_{110} = \frac{I_{110}}{I_{110} + I_{111} + I_{\bar{1}31+041}} \quad (2)$$

$$A_{130} = \frac{I_{130}}{I_{130} + I_{111} + I_{\bar{1}31+041}} \quad (3)$$

$$C = \frac{I_{040}}{I_{110} + I_{040} + I_{130}} \quad (4)$$

B value (earlier known as K value),[25] as a measure for hexagonal β-form content, was calculated by the formula[6] proposed by Zipper et al.[25]:

$$B = \frac{I_{\beta-300}}{I_{\beta-300} + I_{110} + I_{040} + I_{130}} \quad (5)$$

Optical microscopy

A Leica light microscope with digital camera was used for thin crossed microtomed section (1-mm-thick plates) observations. A maximal anisotropic diameter of spherulites ($d_{i,\max}$) was measured on several polarization micrographs of each sample and presented as an average spherulite diameter (d_{sph})

$$d_{\mathrm{sph}} = \frac{\sum N_i d_{i,\max}}{\sum N_i} \quad (6)$$

where N_i is the number of measured spherulites with the average diameter d_i.

Scanning electron microscopy (SEM)

A JEOL JSM-840A scanning electron microscope was used for morphology observation. Samples were fractured in liquid nitrogen and covered with gold before being examined microscopically at an acceleration voltage of 10 kV. All SEM micrographs were taken as secondary electron images.

RESULTS AND DISCUSSION

Structural changes of iPP matrix introduced by incorporation of EPDM and wollastonite

Phase structure and crystallinity

Diffractograms of samples taken by WAXD reveal a prevailing stable monoclinic α-form and small amounts of hexagonal β-form crystalline iPP phase. Typical diffractograms are shown in Figure 1. It is

known that EPDM and wollastonite affect the β-nucleation in the iPP.[4,26,27] Low content of β-phase in the iPP/EPDM blends (with *B* or *K* values for measuring β-form content being 3–4%) indicates that the EPDM elastomer affects β-nucleation insignificantly (Fig. 2). This finding agrees well with the Wenig and Wasiak[26] results, who found only a small amount of β-phase iPP nucleated by EPDM (minimal at 5% of EPDM). The addition of untreated $CaSiO_3$ or treated $CaSiO_3^*$ to the pure iPP increases the *B* values (from 3.3 to 7.4%), thus indicating their influence upon β-nucleation in the iPP matrix (Fig. 2). This result is in accordance with the Liu et al. observation,[4] who discovered that the content of β-iPP might grow up to 37%, if wollastonite of up to 17.7 vol % was added. The addition of wollastonite to the iPP/EPDM blends leads to an increase of β-phase content, which is more regular in iPP/EPDM/$CaSiO_3$ than that in the iPP/EPDM/$CaSiO_3^*$ composites. The overall degree of expectable crystallinity decreases upon the incorporation of the amorphous EPDM into the iPP matrix (Fig. 3). The degree of crystallinity slightly increases with the addition of both wollastonite types to the pure iPP (Fig. 3) and to the iPP/EPDM blends; more regular increase of the degree of crystallinity by the incorporation of untreated wollastonite in the iPP/EPDM blends (iPP/EPDM/$CaSiO_3$) is presented in Figure 4. This effect could be explained by (1) β-nucleation caused by wollastonite increases the amount of β-iPP phase and, consequently, the overall crystallinity; (2) dissolution of amorphous iPP matrix by wollastonite and EPDM (stronger effect at higher EPDM amounts); and/or (3) limiting resolution of applied method.

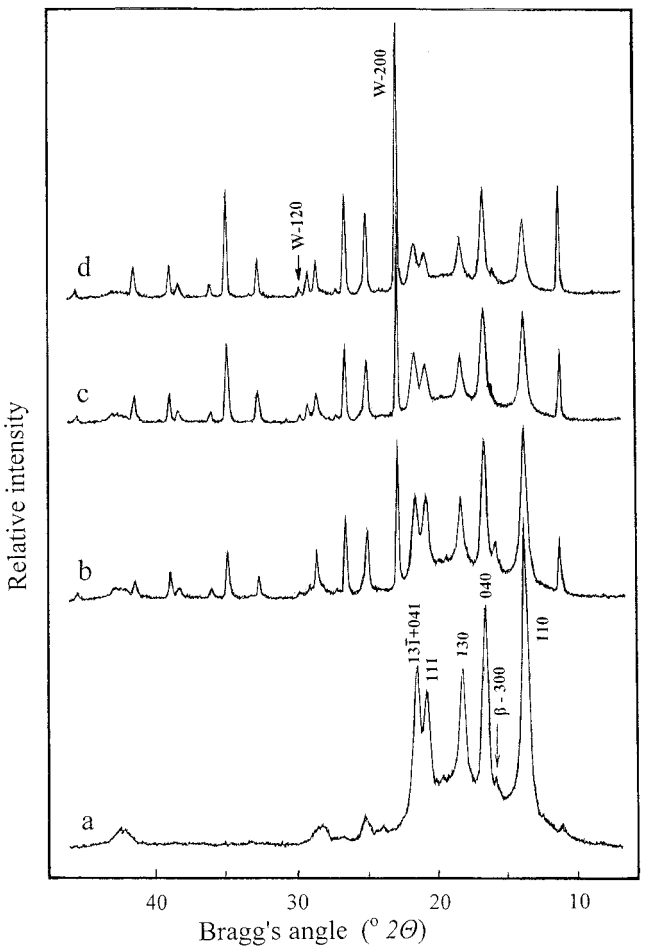

Figure 1 Diffractograms of iPP/EPDM/$CaSiO_3$ composites with 15 vol % EPDM and with added (a) 0 vol %; (b) 2 vol %; (c) 4 vol %; and (d) 6 vol % of untreated $CaSiO_3$.

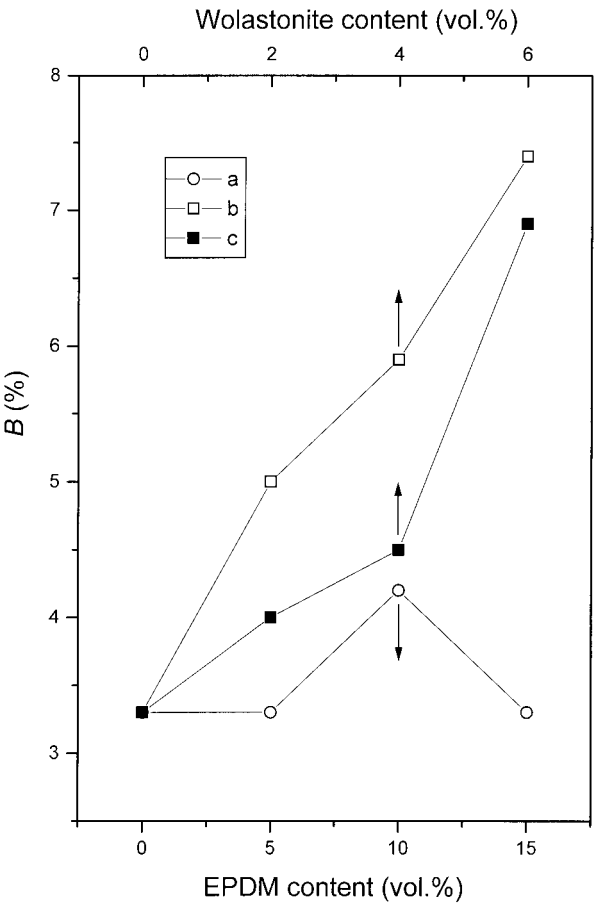

Figure 2 *B* parameter of (a) iPP/EPDM blends, binary (b) iPP/$CaSiO_3$, and (c) iPP/$CaSiO_3^*$ composites as a function of the EPDM or wollastonite content.

Crystallite size

The incorporation of wollastonite into iPP causes a more pronounced increase in the crystallite L_{040} size than that induced by the addition of EPDM (Fig. 5). The values of crystallite L_{040} sizes for both binary iPP/$CaSiO_3$ and iPP/$CaSiO_3^*$ composites are similar. At lower amounts of EPDM (5 vol %), dispersed EPDM particles (acting as heterogeneous nuclei) are smaller and cause an increase in the heterogeneous nuclei density and a decrease in the L_{040} crystallite

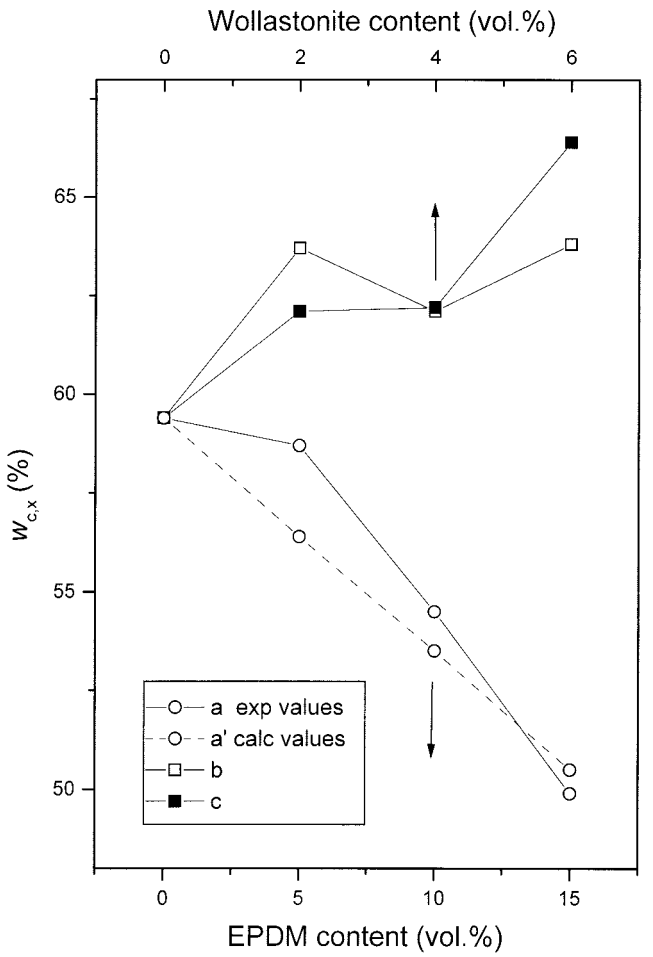

Figure 3 Overall degree of crystallinity, $w_{c,x}$, for iPP/EPDM blends: (a) experimental values and (a′) calculated values, and $w_{c,x}$ for (b) iPP/$CaSiO_3$ and for (c) iPP/$CaSiO_3^*$ composites as a function of the EPDM or wollastonite content.

size. This result agrees with the conclusion that the iPP blending with EPDM reduces lamellar thickness and leads to less perfect crystals.[15,28] Further addition of EPDM (above 5%) causes a steady increase of the L_{040} crystal size. The above increase of crystallite size might be ascribed to the solidification effect, which prolongs crystallization in the iPP/EPDM blends as well as to the easier migration of iPP chains transferred by EPDM melt during the crystallization process. These effects prevail the EPDM nucleation effect and, consequently, enhance crystal growth. When adding atactic polystyrene (aPS), poly(styrene-*b*-butadiene-*b*-styrene) (SBS), and poly(styrene-*b*-ethylene-*co*-propylene) (SEP) to the pure iPP and to the iPP/aPS blends,[29–31] we have observed the analogous crystallite size behavior.

To simplify their graphic illustration and because of their almost identical values in crystallite sizes for ternary composites, we have represented three curves by a single one with the average L_{040} values which depend on the wollastonite content (dotted lines in Fig. 5). The lowest addition of wollastonite (2 vol %), either to the iPP/EPDM blends or to the pure iPP increases the L_{040} crystallite size significantly (Fig. 5). Further addition of filler causes negligible changes of the L_{040} crystallite size. The untreated $CaSiO_3$ causes a somewhat higher L_{040} crystallite size of ternary composites than the treated $CaSiO_3^*$ by adding a 6 vol % of filler (Fig. 5). The addition of wollastonite to the iPP and iPP/EPDM blends influences β-nucleation, and therefore, one may expect the filler to cause the α-form nucleation to decrease the crystal sizes. The opposite result indicates that wollastonite does not affect the nucleation in the iPP matrix only. It seems that the incorporation of both fillers into the iPP and iPP/EPDM blends gradually changes a well-developed spherulitic morphology of the iPP matrix (supported by polarizing microscopy) and favoring the crystal growth of α-form iPP. Close L_{040} values for binary iPP/wollastonite and for ternary iPP/EPDM/wollastonite composites indicate that the increase of crystallite L_{040} size in ternary composites has been caused primarily by the wollastonite addition (i.e., by changes introduced into the iPP matrix spherulitic morphology).

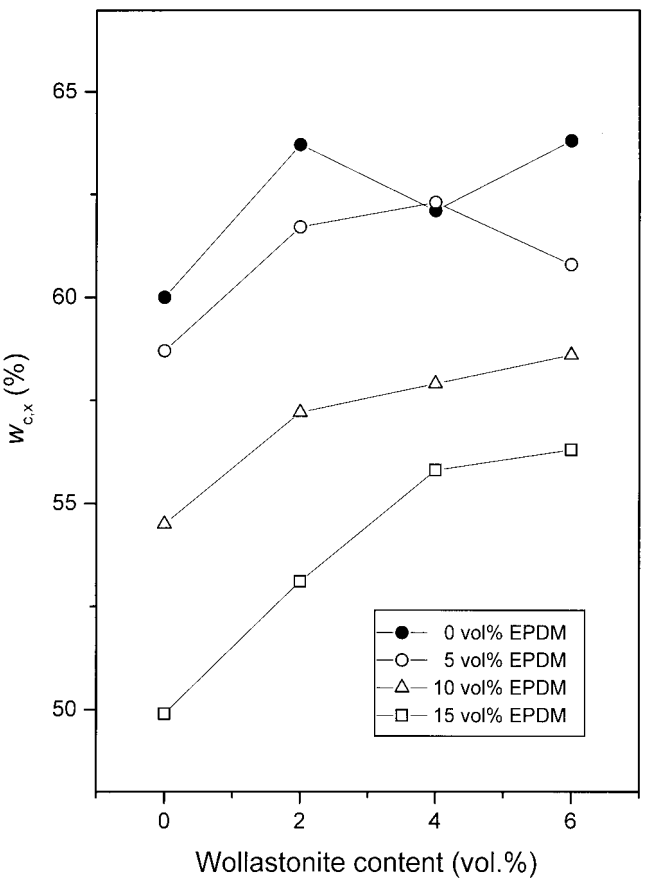

Figure 4 Overall degree of crystallinity, $w_{c,x}$, as a function of wollastonite content for the iPP/EPDM/$CaSiO_3$ with 0, 5, 10, and 15 vol % of EPDM.

Orientation of α-iPP crystallites

The addition of both components (EPDM and filler) changes the intensity relationships of the iPP α-phase reflections (as can be seen from Fig. 1) and, consequently, modifies the A_{110} and A_{130} orientation parameters and C values. Figure 6 shows a small effect of the untreated $CaSiO_3$ and treated $CaSiO_3^*$ fillers on the value of orientation A_{110} parameter. Opposite to the filler incorporation, the addition of 5 and 10 vol % of EPDM to iPP suppresses *110* peak considerably and decreases the value of A_{110} parameter significantly. The addition of 15 vol % of EPDM returns the A_{110} value to at least the one of the original iPP. The obtained V or U shapes of the A_{110} (curve a in Fig. 6), resembling a similar shape of the L_{040} (curve a in Fig. 5) for iPP/EPDM blends, might be caused by nucleation and chain transferring abilities of the EPDM in the iPP matrix crystallization process. Because of very similar A_{110} values of ternary composites, one with average A_{110} values represents three close curves dependent on EPDM content (dotted lines in Fig. 6). The intermediate position of the A_{110} curves for ternary composites (curves d, e in Fig. 6) between those for binary systems indicates that there has been a combined influence of both elastomer and filler on the A_{110} orientation parameter. Similar influence exhibits the incorporation of elastomer and filler to the A_{130} parameter.

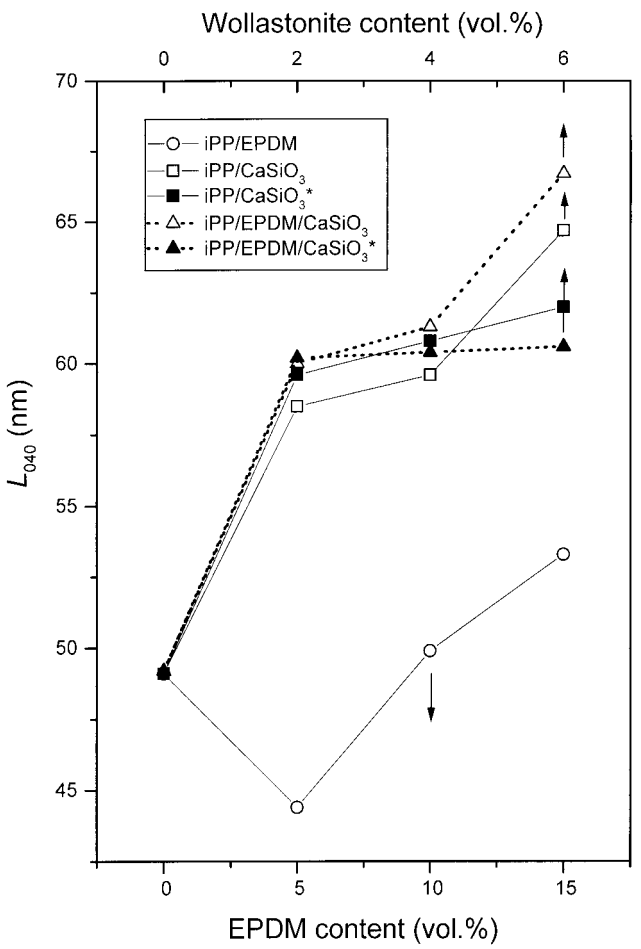

Figure 5 Crystallite size, L_{040}, as a function of the EPDM and wollastonite content for (-○-) iPP/EPDM blends, (-□-) iPP/$CaSiO_3$, and (-■-) iPP/$CaSiO_3^*$ composites, and average these values for ternary composites with (-△-) $CaSiO_3$ and (-▲-) $CaSiO_3^*$.

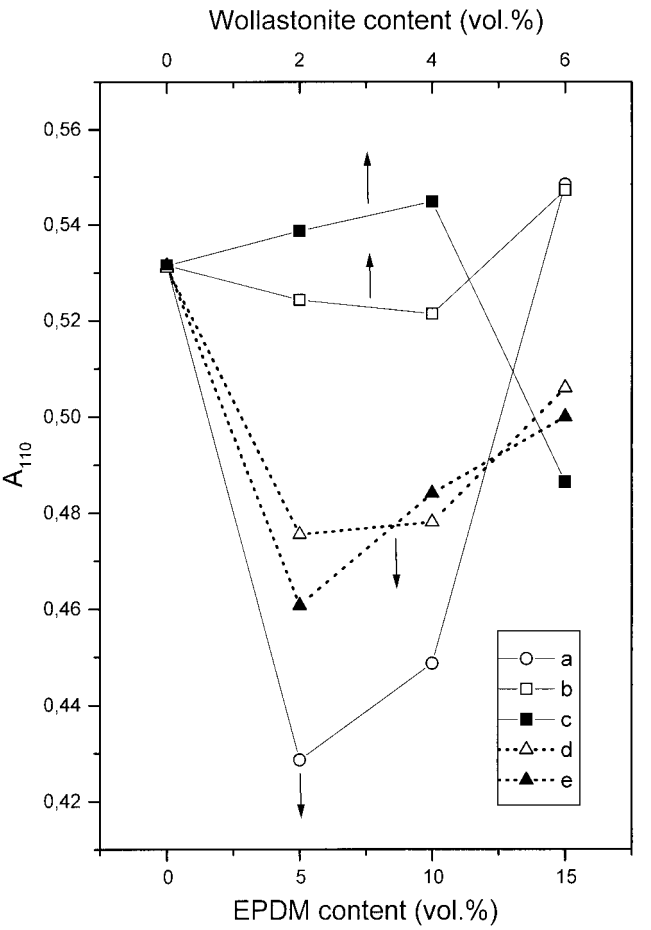

Figure 6 Orientation A_{110} parameter as a function of the EPDM or wollastonite content for (a) iPP/EPDM blends, (b) iPP/$CaSiO_3$, and (c) iPP/$CaSiO_3^*$ composites, and the average of these values for ternary composites with (d) $CaSiO_3$ and (e) $CaSiO_3^*$.

Different effects of EPDM and filler on the C parameter are shown in Figure 7. On one hand, the addition of EPDM to the iPP affects the C parameter negligibly, and on the other, the addition of both wollastonites to the iPP increases the C values significantly. Close C values of ternary iPP/EPDM/$CaSiO_3$ and iPP/EPDM/$CaSiO_3^*$ composites are represented by dotted curves with average C values dependent upon wollastonite content. Analogously to the A_{110} and A_{130} parameters, the average C curves of ternary composites take intermediate positions between those for binary systems (Fig. 7).

In general, wollastonite increases the C index mainly, which implies the increase of a^*-axis orientation, because, according to Zipper et al., $C = 1$ for pure

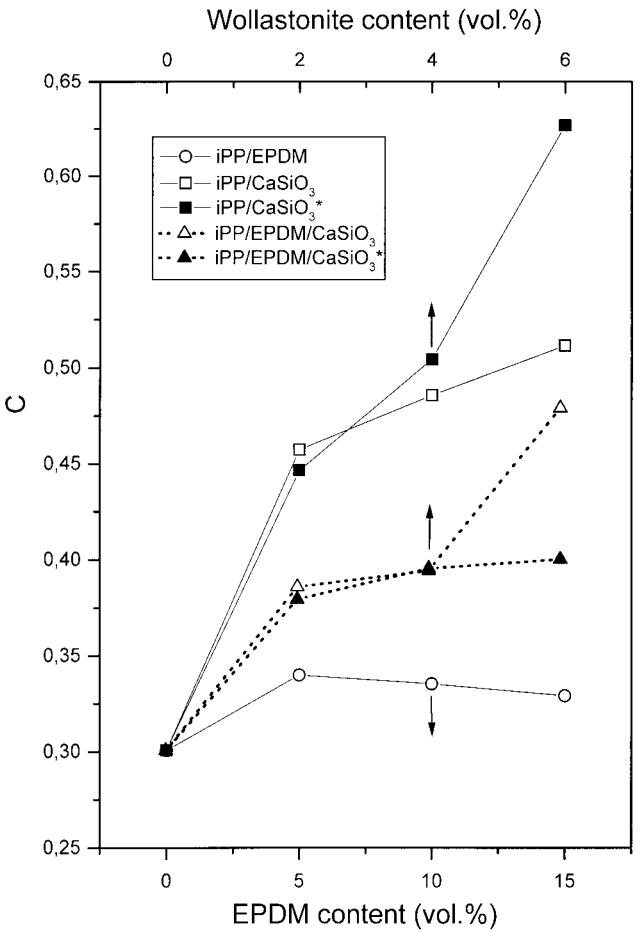

Figure 7 Orientation C parameter as a function of the EPDM and wollastonite content for (-○-) iPP/EPDM blends, (-□-) iPP/$CaSiO_3$ and (-■-) iPP/$CaSiO_3^*$ composites, and average C values for ternary composites with (-△-) $CaSiO_3$ and (-▲-) $CaSiO_3^*$.

*a**-axis orientation.[25] According to Lovinger,[32] *a** is the axial direction of lamellar growth and preferred radial growth of spherulites. Moreover, according to Fujiyama et al.,[33] *a**-axis-oriented lamellae are the planes parallel to the sample surface. The as-included wollastonite crystals cause an increase in the number of plan-parallel *a**-axis-oriented α-iPP lamellae. On the other hand, the *C* values, which remained low even upon the addition of EPDM to iPP, might be explained by maintaining either *c*-axial orientation or isotropic iPP matrix ($0 < C \ll 1$ for pure *c*-axis orientation or for isotropic material).[25] A significant decrease of A_{110} parameter after adding lower EPDM amounts indicates, according to Trotignon and Verdu[24] and Zipper et al.[25] ($A_{110} = 1$ when 110 planes are parallel to the surface; $A_{110} = 0$ for every other orientation), however, a reorientation influence of EPDM, which decreases the number of crystal 110 planes of α-iPP inplane parallel to the sample surface. It seems that EPDM increases a *c*-axis-oriented α-iPP lamellae. The intermediate positions of the A_{110} and A_{130} orientations and *C* parameters for ternary composites (Figs. 6 and 7) are indicative of the influence of both elastomer and filler on these parameters and do so in two possible ways: (1) combined influence of the EPDM dispersed particle and filler, and (2) by partial encapsulation of filler by EPDM.

Phase morphology

Effect of elastomer and fillers on spherulitic morphology

Polarization micrographs in Figure 8 show the increase of well-developed spherulites with the addition of EPDM elastomer to the pure iPP. A uniform spherulitic morphology over the entire cross sections of each sample consists predominantly of radial α-spherulites. By the incorporation of wollastonite into pure iPP, the spherulite size decreases gradually; very small flower-like spherulites can be seen from polarizing micrographs in Figure 9. On some micrographs of ternary composites with 6 vol % of both fillers, the spherulites of the same level size may be

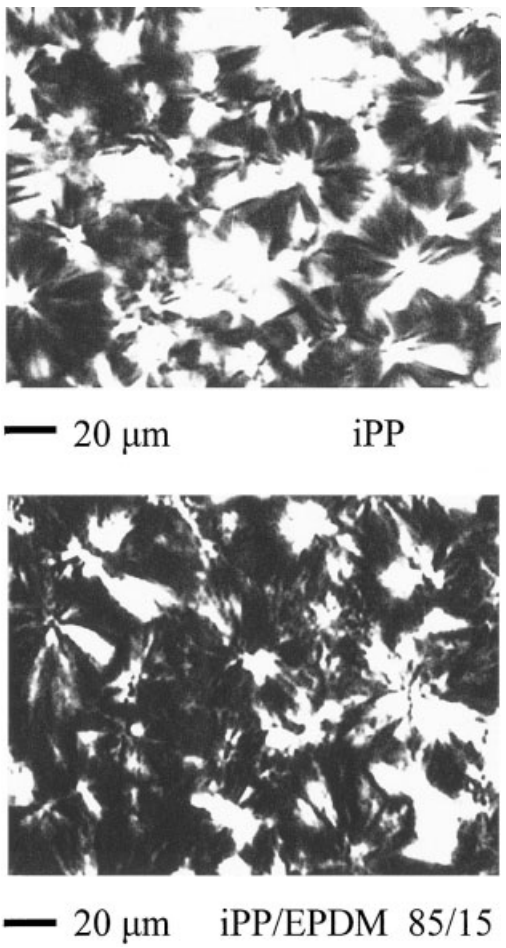

Figure 8 Polarizing micrograph of iPP/EPDM 85/15 blend compared to one of the pure iPP.

recognized; however, the resolution is so indistinct that the spherulite size is immeasurable. Figure 10 shows a significant increase in spherulite size upon the addition of EPDM to the pure iPP. The maximum is reached at 10 vol % of EPDM. Analogous increase of spherulite size has been observed in the iPP/SBS and iPP/SEP blends.[30,31] Wenig and Wasiak[26] explained maximal growth rate of spherulites and minimal glass transition temperature in the iPP/EPDM blends at a 10 vol % EPDM content by the degree of EPDM dispersion and thermodynamic origin of interactions between EPDM and iPP chains in interface layer.

The addition of both wollastonites, especially untreated $CaSiO_3$, gradually causes a decrease of the spherulite size, as shown in Figure 10. Due to nucleation ability of long needle-like wollastonite crystals, the growth of well-developed spherulites is disturbed. Thinner spherulites may be as well the outcome of an interaction between wollastonite and iPP matrix, resulting in favored growth of orientated iPP lamellae. The addition of treated $CaSiO_3^*$ causes the appearance of larger spherulites rather than the addition of untreated $CaSiO_3$ to the pure iPP (d_{sph} = 48 μm in comparison to d_{sph} = 33 μm) and to the iPP/EPDM 85/15 blend (d_{sph} = 53 μm in comparison to d_{sph} = 43 μm) (Fig. 10). The spherulites grow with the addition of EPDM up to 10 vol % to the binary iPP/$CaSiO_3$ composites. It seems that the addition of EPDM elastomer compensates the nucleation effect of untreated wollastonite.

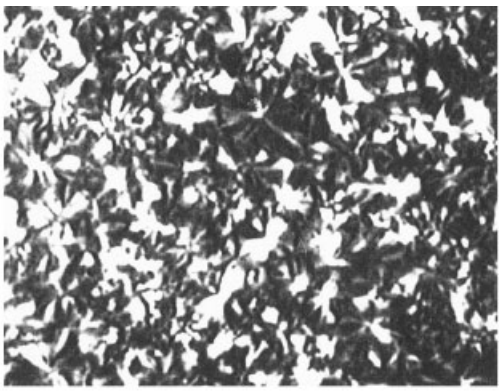

Figure 9 Comparison of spherulitic morphology of binary iPP/$CaSiO_3$ 98/2 composites with ternary iPP/EPDM/$CaSiO_3$ 88/10/2 composites represents with polarizing micrographs.

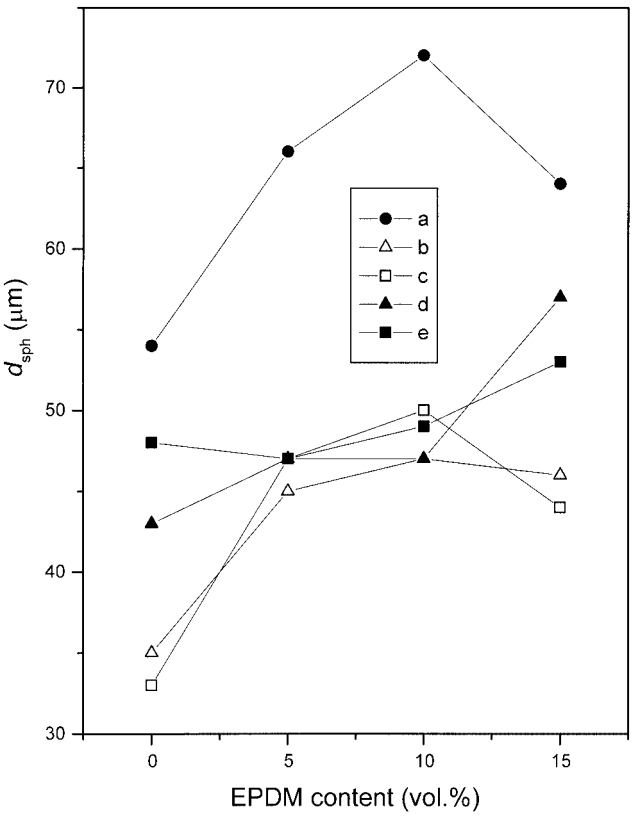

Figure 10 Maximal diameter of spherulites for (a) iPP/EPDM blend, and iPP/EPDM/$CaSiO_3$ composites with (b) 2 vol % and (c) 4 vol % of $CaSiO_3$, as well as iPP/EPDM/$CaSiO_3^*$ composites with (d) 2 vol % and (e) 4 vol % of $CaSiO_3^*$.

Inclusion of wollastonite crystals and dispersed EPDM particles

Acicular wollastonite crystals are dispersed in iPP matrix homogeneously without agglomeration and clustering, as can be seen from Figure 11(a, b). Optical and SEM micrographs also reveal their predominantly plan-parallel alignment toward the sample surface. X-ray patterns of both applied wollastonites are closer to the Card No. 27-1064 [triclinic cell with space group $PF\bar{1}$ (2T)][34] than to the Card No. 19-249 [triclinic cell with space group P1 (1T)].[35] The intensities of some wollastonite reflections, especially the *120* peak, in the diffractograms of the composites change in compari-

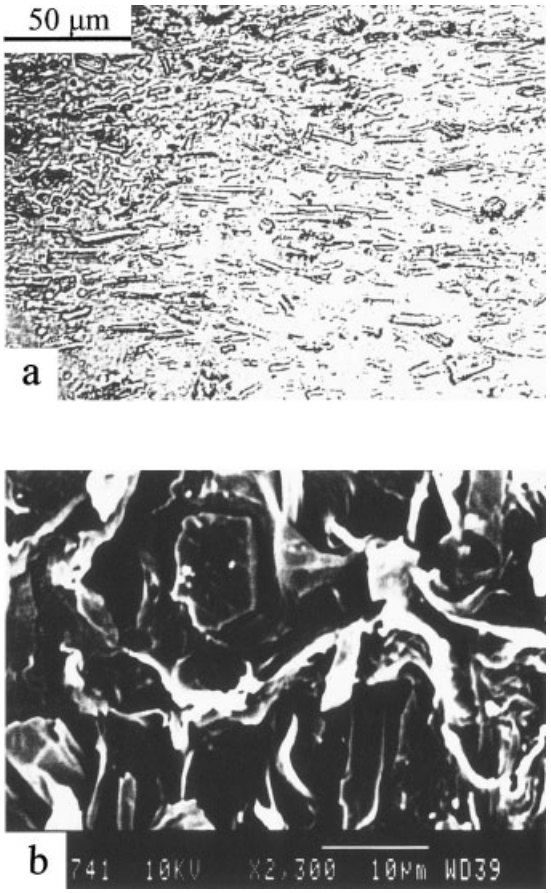

Figure 11 Optical micrograph of (a) horizontal cross section of iPP/$CaSiO_3^*$ 98/2 composite and scanning electron micrograph of (b) vertical cross section of iPP/$CaSiO_3$ 94/6 composite; wollastonite crystals are oriented plan-parallel to the surface of each sample.

son to the diffractograms of pure $CaSiO_3^*$ and $CaSiO_3$. Behavior of intensity relationships of *120* and *200* reflections (Fig. 12) confirms the preferential orientation of wollastonite crystals incorporated into the iPP matrix. A slight increase of the intensity relationship upon the EPDM addition indicates a slight reorientation of wollastonite crystals caused by decreasing of melt viscosity and/or interaction between wollastonite crystals and EPDM elastomer.

Fine spherical EPDM particles with relatively narrow size distribution (estimated from the SEM micrographs $d_p = 0.2 \cdots 1.3$ μm for iPP/EPDM 95/5; $d_p = 0.3 \cdots 2.0$ μm for iPP/EPDM 90/10) are randomly dispersed within the iPP matrix, as can be seen from Figure 13. At a higher amount of EPDM (up to 15 vol %), the dispersed EPDM particles coalesce in forms with more irregular shapes.

Morphology of ternary iPP/EPDM/wollastonite composites

Polarization and optical micrographs of pure iPP, iPP blends, and composites exhibit uniform spherulitic morphology along the entire cross section of samples without skin-core effect (without morphological layers). Encapsulation of the wollastonite crystals with the added EPDM elastomer might be expected because of its lower viscosity if compared to iPP, and possible interactivity of polybutadiene chains in EPDM and filler surface. Although the influence of EPDM on wollastonite orientation in the iPP matrix (Fig. 12) may be explained by the melt viscosity change, reduced ability of the filler to orient the iPP crystallite with the EPDM addition indicates possible acting of EPDM as an interlayer between wollastonite and iPP. Moreover, wollastonite crystals still present on the fractured composites surface and some of them constrained in dark hollows (as shown in the SEM micrographs in Figs. 14 and 15) may indicate the encapsulation of wollastonite crystals by elastomer. However, only seldom do wollastonite crystals exhibit core–shell morphology as shown in Figure 15. Most of the elastomer in ternary composites is predominantly dispersed into iPP matrix because of the similarity of the EP chain segments and PP chains and/or interactions between double bonds of dienes and iPP chains (Figs. 14 and 15). It is also possible that acicular habit of long

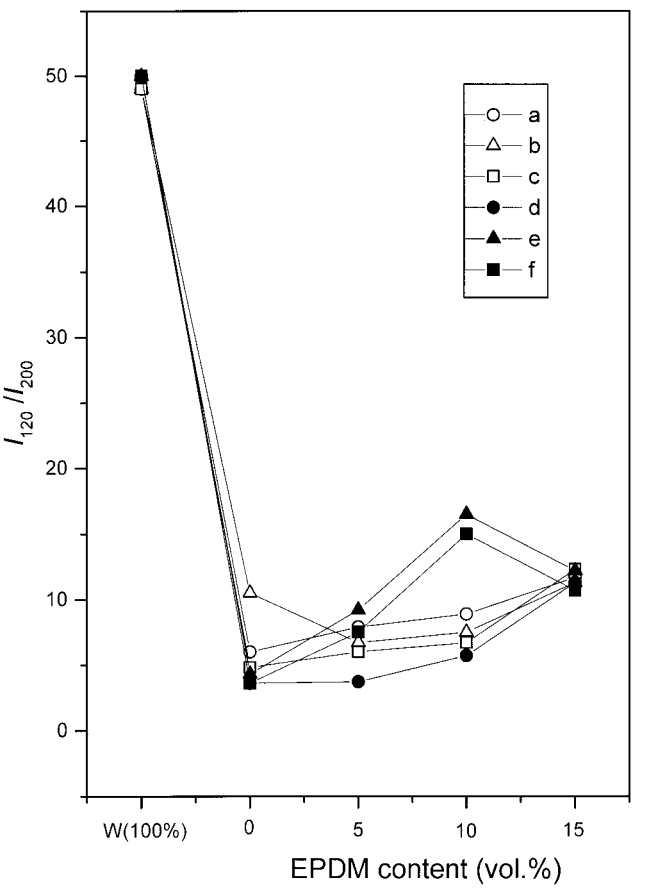

Figure 12 Intensity relationship I_{120}/I_{200} of wollastonite reflections for ternary iPP/EPDM/W composites with (a) 2 vol %, (b) 4 vol %, and (c) 6 vol % of $CaSiO_3$ and with (d) 2 vol %, (e) 4 vol %, and (f) 6 vol % of $CaSiO_3^*$.

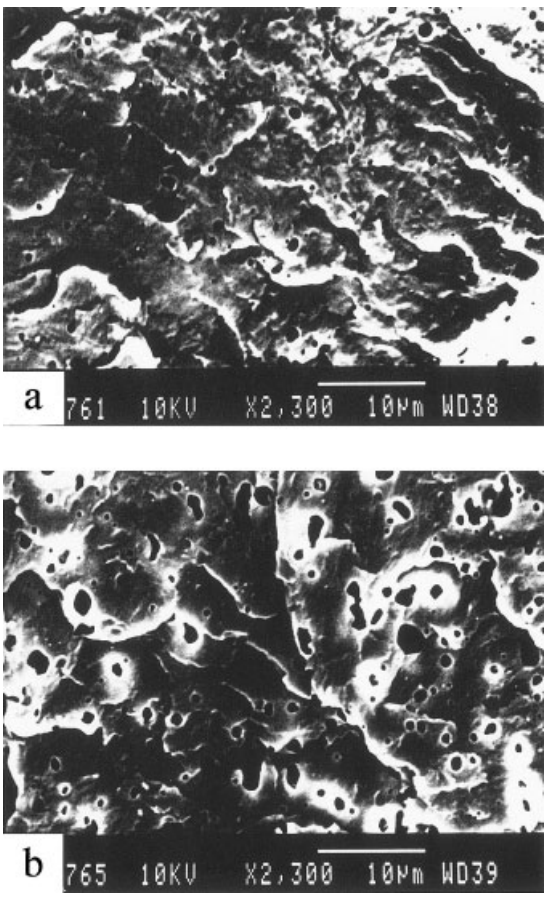

Figure 13 Scanning electron micrographs of the fractured surfaces of iPP/EPDM blends with (a) 90/5 and (b) 85/15 volume ratios.

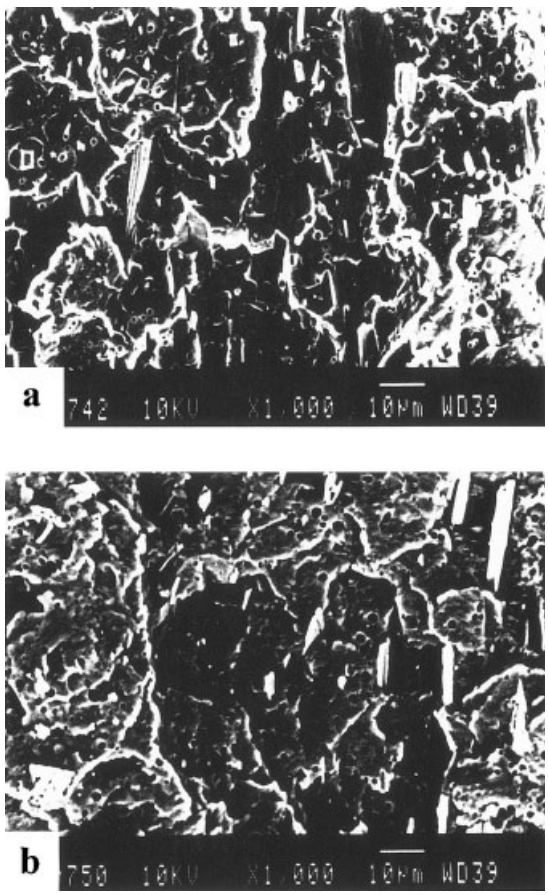

Figure 14 Scanning electron micrographs of the fractured surfaces (a) iPP/EPDM/$CaSiO_3$ 89/5/6 and (b) iPP/EPDM/$CaSiO_3^*$ 89/5/6 composites.

wollastonite crystals hinders their encapsulation by EPDM elastomer.

The factors influencing final structure of iPP blends and composites

The characteristics of filler and dispersed elastomer particles as well as the interfacial adhesion between polymer matrix and ingredients primarily influence impacting of an amorphous polymer composite. However, in the case of semicrystalline polymer (such as isotactic polypropylene), the changes in supermolecular structure are important for the impacting of such composite. Untreated $CaSiO_3$ crystals affect the β-iPP phase more efficiently than treated $CaSiO_3^*$ in the iPP composites. High increase of β-phase content for the composites with untreated $CaSiO_3$ contributes to higher overall degree of crystallinity. Untreated $CaSiO_3$ also affects crystal growth in the 040 direction and decreases the spherulite size more than treated $CaSiO_3^*$. Obviously, uncoated $CaSiO_3$ crystals affect crystallization processes in the iPP matrix more strongly than coated $CaSiO_3^*$. As was previously reported,[11,13] polypropylene composites with uncoated wollastonite exhibited higher impact strength than that one with coated filler. This difference in toughness is in accordance with differences in the final supermolecular structure of the iPP composites described in this work and could be explained by several factors, as follows.

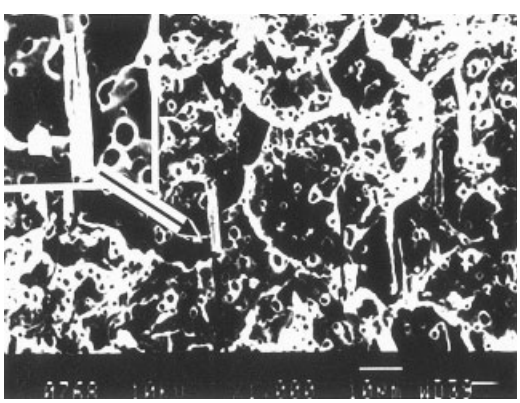

Figure 15 Scanning electron micrographs of the fractured surfaces iPP/EPDM/$CaSiO_3$ 81/15/4 composite; inserted figure illustrates encapsulated wollastonite crystal.

(1) Polypropylene melt may penetrate into pores, cavities, and other irregularities on the rough surface of uncoated $CaSiO_3$ crystals, promoting mechanical connections. Aminosilanes, used as a surface modifier for wollastonite, reduce the surface roughness and separate $CaSiO_3$ surface from the iPP matrix and spreads stress concentrations from the $CaSiO_3$–iPP interface to the aminosilanes–iPP interface. It seems that the aminosilanes–iPP interfacial adhesion is rather weak.

(2) The uncoated $CaSiO_3$ crystals cause the formation of smaller spherulites than coated $CaSiO_3^*$ crystals. iPP matrix with smaller spherulites may contribute to the higher impact strength of iPP composites.

(3) The uncoated $CaSiO_3$ filler enhances β-iPP phase content. iPP composites with higher β-iPP content consist of tougher iPP matrix as a result of higher impact strength of sheaf-like β-iPP spherulites compared to radial α-iPP spherulites.[36]

Generally, EPDM terpolymer should act as an impact modifier for iPP matrix and as a compatibilizer (coupling agent) between wollastonite filler and iPP matrix. EPDM elastomer acts as a strong impact modifier for polypropylene. Presented results show only part encapsulation of wollastonite filler (somewhat expressive for uncoated $CaSiO_3$) by EPDM elastomer. The main part of the elastomer is dispersed into iPP matrix of the composite due to the similarity of the EP segments and iPP chains and interactions between dienes and iPP chains. Optimal compatibilizer for coated $CaSiO_3^*$ should be interacted or mixed with aminosilane chains on the $CaSiO_3^*$ surface.

CONCLUSION

Supermolecular structure of polypropylene blends and composites is affected differently by the incorporation of the EPDM elastomer and wollastonite fillers. The addition of EPDM strongly increases the spherulite size (transferring ability), whereas the addition of both wollastonites gradually decreases it (nucleation ability). Furthermore, the filler affects the nucleation of the β-form iPP and the crystal growth of α-form is stronger than the EPDM terpolymer. Plan-parallel accommodation of long acicular wollastonite crystals hinders a well-developed spherulitization and increases the number of the a^*-axis-oriented α-iPP lamellae. On the other hand, it seems that EPDM increases the c-axis orientation of the α-iPP lamellae. The intermediate values of A_{110}, A_{130}, and C orientation parameters for ternary composites result from the combined influence of both elastomer and filler. The difference between two filler types manifests in their effects upon the spherulite size. The addition of treated $CaSiO_3^*$ to the pure iPP and to the iPP/EPDM blend with higher EPDM content causes the growth of larger spherulites than those obtained by the addition of untreated $CaSiO_3$.

The Ministry of Science and Technology of the Republic of Slovenia and the Ministry of Science and Technology of the Republic of Croatia have financially supported this work. The authors thank Dr. N. Filipović-Vinceković for useful advice when writing this article and J. Pohleven for help in the experimental work.

References

1. Kietzman, J H. in Additives for Plastics; Seymour, R. B., Ed.; Academic Press: New York, 1978; Vol. 1, pp. 51–77.
2. Rothon, R. N. Adv Polym Sci 1999, 139, 67.
3. Wypich, G. Handbook of Fillers; SPE: New York, 1999; pp. 167–169.
4. Liu, J.; Wei, X.; Guo, Q. J Appl Polym Sci 1990, 41, 2829.
5. Jilken, L. Polym Testing 1991, 10, 329.
6. Trotignon, J. P.; Demdoum, L.; Verdu, J. Composites 1992, 23, 313, 319.
7. Shen, J.; Ji, G.; Hu, B.; Huang, Y. J Mater Sci Lett 1993, 12, 1344.
8. Gaskel, P.; Smith, A. C. Plast, Rubber Compos Process Appl 1994, 22, 171.
9. Järvela, P. A.; Järvela, P. K. J Mater Sci 1996, 31, 3853.
10. Vinci, M.; La Mantia, F. P. J Polym Eng 1996/7, 16, 203.
11. Roberts, D. H. In Conference Proceedings at ANTEC'98: Plastics on my Mind; Atlanta, Apr 26–30 1998; SPE: Brookfield, pp. 1427–1431.
12. Chu, J.; Rumao, L.; Coleman, B. Polym Eng Sci 1998, 38, 1906.
13. Wong, T. L.; Barry, M. F.; Orroth, S. A. J Vinyl Additive Technol 199, 5, 235.
14. Chu, J.; Xiang, C.; Sue, H.-J.; Hollis, R. D. Polym Eng Sci 2000, 40, 944.
15. Pukanszky, B.; Tüdös, F.; Kallo, A.; Bodor, G. Polymer 1989, 30, 1399.
16. Bartczak, Z.; Martuscelli, E.; Galeski, A. in Polypropylene: Structure Blends and Composites, Vol. 2: Copolymers and Blends; Karger-Kocsis, J., Ed.; Chapman and Hall: London, 1995; Chapter 2.
17. Monasse B.; Haudin, J. M. in Polypropylene: Structure Blends and Composites, Vol. 1: Structure and Morphology; Karger-Kocsis, J., Ed.; Chapman and Hall: London, 1995; Chapter 1.
18. Pukanszky, B.; Tüdös, F.; Kolarik, J.; Lednicky, F. Polym Composites 1990, 11, 98.
19. Chiang, W. Y.; Yang, W. D. Polym Eng Sci 1992, 32, 641.
20. Schaefer, K. U.; Theisen, A.; Hess, M.; Kosfeld, R. Polym Eng Sci 1993, 33, 1009.
21. Weidinger, A.; Hermans, P. H. Makromol Chem 1961, 44, 98.
22. Gedde, U. W. Polymer Physics; Chapman and Hall: London, 1995; Chapter 7, p. 157.
23. Alexander, L. E. X-ray Diffraction Methods in Polymer Science; Wiley: New York, 1969; Chapter 7.
24. Trotignon, J. P.; Verdu, J. J Appl Polym Sci 1987, 34, 1.
25. Zipper, P.; Janosi, A.; Wrentschur, E. J. Physique IV, Suppl J Phys I 1993, 3, 33.
26. Wenig, W.; Wasiak, A. Colloid Polym Sci 1993, 271, 824.
27. Varga, J. Crystallization, Melting and Supermolecular Structure of Isotactic Polypropylene in Polypropylene: Structure, Blends and Composites, Vol. 1: Structure and Morphology; Karger-Kocsis, J., Ed.; Chapman & Hall: London, 1995; Chapter 3.
28. Wlochowicz, A.; Eder, M. Polymer 1984, 25, 1268.
29. Radonjiê, G.; Musil, V.; Šmit, I. J Appl Polym Sci 1998, 69, 2625.
30. Šmit, I.; Radonjiê, G. Polym Eng Sci 2000, 40, 2144.
31. Radonjiê, G.; Šmit, I. J Polym Sci, Polym Phys Ed 2001, 39, 566.
32. Lovinger, A. J. J Polym Sci, Polym Phys Ed 1983, 21, 97.
33. Fujiyama, M.; Wakino, T.; Kawasaki, Y. J Appl Polym Sci 1988, 35, 29.
34. Powder Diffraction File, ICDD, JCPDS, Swarthmore, PA (Card No. 27-1064).
35. Powder Diffraction File, ICDD, JCPDS, Swarthmore, PA (Card No. 19-249).
36. Tjong, S. C.; Shen, J. S.; Li, R. K. Y. Polym Eng Sci 1996, 36, 100.